

Simulations of X–ray spectral/timing properties in a propagation model of variability of accreting black holes

Piotr T. Życki*

Nicolaus Copernicus Astronomical Center, Bartycka 18, 00-716 Warsaw, Poland

23 Nov 2002

ABSTRACT

A phenomenological model of X–ray variability of accreting black holes is considered, where the variable emission is attributed to multiple active regions/perturbations moving radially towards the central black hole. The hard X–rays are produced by inverse Compton upscattering of soft photons coming from reprocessing/thermalization of the same hard X–rays. The heating rate of the Comptonizing plasma is assumed to scale with the rate of dissipation of gravitational energy while the supply of soft photons is assumed to diminish towards the center. Two scenarios are considered: (1) an inner hot flow with outer truncated standard accretion disc and (2) an accretion disc with an active corona and a thick hot ionized skin. A variant of the model is also considered, which is compatible with the currently discussed multi-Lorentzian description of power spectral densities of X–ray lightcurves.

In the inner hot flow scenario the model can reproduce the observed Fourier frequency resolved spectra observed in X–ray binaries, in particular the properties of the reprocessed component as functions of Fourier frequency. In the accretion disc with ionized skin scenario the reduction of soft photons due to the ionized skin is insufficient to produce the observed characteristics.

Key words: accretion, accretion disc – instabilities – stars: binary – X–rays: general – X–rays: stars

1 INTRODUCTION

X–ray emission from accreting compact objects carries information about geometry and physical conditions of the accreting plasma. Spectral and timing analyses of the data from sources in low/hard state have enabled formulating a number of phenomenological scenarios for accretion onto black holes. The scenarios belong to two main groups: (1) models invoking standard optically thick accretion disc with an active corona and (2) models assuming that the optically thick disc is truncated at a radius larger than the last stable orbit, and is replaced by inner hot, optically thin flow (see Done 2002, Czerny 2002 for reviews). Models of both groups have some physical foundations. Magnetic dynamos in the disc may give rise to the active corona, as suggested by recent magneto-hydrodynamical simulations (Miller & Stone 2000), with plasma outflow and/or hot ionized disc skin responsible for the observed correlations between spectral parameters: the power law slope and amplitude of the reflected component (Zdziarski, Lubiński & Smith 1999; Gilfanov, Churazov & Revnivtsev 2000); On the other hand, disap-

pearance of the cold disc due to evaporation may create the inner hot flow (Różańska & Czerny 2000). Both classes of models can explain time average energy spectra, as well as correlations between spectral parameters (see discussion of models and more references in Życki 2002; hereafter Z02).

Specific models of X–ray variability were constructed for both geometries (see Poutanen 2001 for review). In the active corona geometry the model of magnetic flare avalanches of Poutanen & Fabian (1999; hereafter PF99) is very successful in reproducing a number of observed properties (e.g. power spectra, hard X–ray time lags). However, its simple extension to accretion disc with the ionized skin fails to reproduce the Fourier-frequency resolved spectra (Revnivtsev, Gilfanov & Churazov 1999, 2001) observed from black hole binaries (Z02). In the inner hot flow geometry the drifting blob model (Böttcher & Liang 1999) reproduces certain observed characteristics. However, Maccarone, Coppi & Poutanen (2000) argue that flares in hard (Comptonized) X-rays are the primary driver of variability, the soft (thermal) emission being merely reprocessed hard X-rays (see also Malzac & Jourdain 2000).

The observed logarithmic energy dependence of the hard X–ray time lags was shown to be compatible with a

* e-mail: ptz@camk.edu.pl

simple propagation model, where X-ray emitting perturbations move radially towards the central black hole, the emitted spectrum hardening as the perturbations approach the center (Miyamoto & Kitamoto 1989; Nowak et al. 1999; Kotov, Churazov & Gilfanov 2001). Moreover, the observed characteristic 'dip' in the energy dependence of time lags at the energy of the Fe K α line can be explained in the propagation model, if the line emission from inner disc is suppressed (Kotov et al. 2001).

Therefore in this paper we consider a phenomenological propagation model, where the variable X-ray emission is attributed to active regions and/or perturbations moving radially towards the central compact object. X-rays are assumed to be produced by inverse Compton upscattering of soft photons coming from a cool, optically thick disc. X-ray luminosity is assumed to increase as the emission progresses, thus creating a flare of radiation. The Comptonized spectrum is assumed to evolve from softer to harder during the flare due to diminishing supply of seed photons. This may be due to either the optically thick disc being absent at small radii, or the thickness of the ionized disc skin increasing towards the center. From the simulated event files a number of statistics will be computed, which may be compared to available data. In particular, the Fourier-frequency resolved spectral properties are studied: both the continuum slope and Fe K α line strength as functions of Fourier frequency, f , will be computed. The observed Fourier-frequency resolved spectra, calculated from the *RXTE* data of black hole binaries in the low/hard state, show two important characteristics: the continuum spectra get harder with increasing f , while the amplitude of reflection decreases with f (Revnivtsev et al. 1999, 2001).

We emphasize that the main feature of the considered models is the radial propagation of the X-ray emitting structures, with the related spectral evolution. This is meant to be compared with the models assuming radially localized flares (e.g. the model of PF99). However, we do not hypothesize here about possible correlations between flares (although the idea of flare avalanches will be implemented in Sec 3.2), hence this model is not meant to explain in detail the X-ray power spectra and higher order statistics of the variability (Maccarone & Coppi 2002).

Plan of the paper is as follows: the model is described in Sec. 2, results for the hot inner flow geometry are presented in Sec. 3, while results for the case of an accretion disc with hot ionized skin are presented in Sec. 3.3. In Sec. 4 a variant of the model is considered, which is compatible with the multi-Lorentzian description of power spectra (Nowak 2000).

2 THE MODEL

The X-ray emitting structures are assumed to originate at a certain radius r_{out} , which will be assumed $\sim 50 r_g$ ($r_g \equiv GM/c^2$; precise value of r_{out} has little influence on our results, since the contribution to emission from large distances is insignificant). They move towards the center at a fraction of the free-fall speed,

$$v = \beta v_{\text{ff}} = \beta \sqrt{\frac{2GM}{r}}, \quad (1)$$

where β is a model parameter. Since the heating of the plasma must ultimately come from the dissipation of the gravitational energy, we assume that the plasma heating rate scales as the dissipation rate of the latter for a disc-like accretion,

$$l_{\text{h}}(t) \propto r(t)^{-2} b[r(t)], \quad (2)$$

where the exponent -2 corresponds to dissipation per ring of matter. Here l is the compactness parameter, $l \equiv \frac{L}{R_{\text{flare}}} \frac{\sigma_{\text{T}}}{m_e c^3}$ (R_{flare} is the characteristic radius of the structure), and $b(r)$ is the boundary term which is assumed to have its Newtonian form $b(r) = 1 - \sqrt{6} r_g/r$ (Shakura & Sunyaev 1973). Other prescriptions for $l_{\text{h}}(r)$ could be used here, since the relation between the overall disc accretion flow and the motion of structures is obviously uncertain¹. The heating rate is normalized to have an assumed maximum value, $l_{\text{h,max}}$. Solving the equation of motion (Eq. 1) gives

$$r(t) = (r_{\text{out}}^{3/2} - At)^{2/3}, \quad (3)$$

where $A = \frac{3}{2} \frac{\sqrt{2}\beta c}{r_g}$, and the radial positions are expressed in units of r_g . The duration of a flare is $t_{\text{trav}} = (r_{\text{out}}^{3/2} - 6^{3/2})/A$, since the final radial position is assumed $6 r_g$. The resulting flare, $l_{\text{h}}(t)$, is characterized by a slow rise and a sudden decrease (Fig. 1a) in agreement with the constraints derived by Maccarone et al. (2000).

The soft photons are assumed to come from reprocessing and thermalization of the hard X-rays, so that the feedback loop is realized as needed to explain the R - Γ correlation (Zdziarski et al. 1999; Gilfanov et al. 2000). Two geometrical scenarios may be considered here:

(i) an inner hot flow partially overlapping a cold, optically thick disc disrupted at certain radius, r_{tr} , (see e.g. Poutanen, Krolik & Ryde, 1997, for arguments for the overlap). The luminosity of soft photons crossing an active region is therefore parametrized as

$$l_{\text{s}}(t) = l_{\text{h}}(t) \times N_{\text{s}} \begin{cases} 1 & \text{for } r \geq r_{\text{tr}} \\ \left(\frac{r}{r_{\text{tr}}}\right)^2 & \text{for } r < r_{\text{tr}}, \end{cases} \quad (4)$$

where $N_{\text{s}} \approx 0.5$,

(ii) a standard optically thick accretion disc with an active corona and a hot ionized skin on top of the disc (Nayakshin & Dove 2001). The flux of soft photons crossing an active region is computed using the method of Życki & Różańska (2001) and Z02, for an assumed height of the active region above the disc, as it travels towards the center.

It should be noted here that for a truncated disc, wholly replaced by a hot flow, and for a compact emission region, the resulting dependence $l_{\text{s}}(r)/l_{\text{h}}(r)$ is much steeper than the assumed r^2 . That is, once the active region is within the

¹ One subtle geometrical effect here is the radial dependence of the size of the emitter, R_{flare} . Actually, it is the luminosity from each emitter that can be expected to scale as r^{-2} . Then, eq. 2 is equivalent to an assumption $R_{\text{flare}} = \text{const}$. If R_{flare} varies with r , radial dependencies of L and l_{h} will be different, but the observed quantity is L and this should scale as r^{-2} . Precise values of $l_{\text{h}}(r)$ is not important in our paper because of approximations used to compute the spectra (eq. 4). In particular, pair production processes are neglected. This problem will be more apparent in Section 3.3.

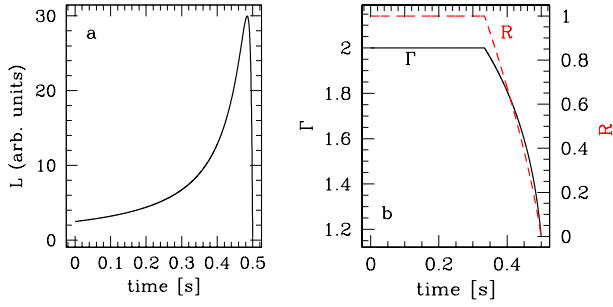


Figure 1. Time variations of parameters during a flare in the truncated disc scenario. (a) luminosity of a flare, (b) spectral index, Γ , and amplitude of reflection, R . Parameters: $r_{\text{out}} = 60 r_g$, $\beta = 0.02$ so that the flare duration is $t_{\text{trav}} = 0.5$ sec, $r_{\text{tr}} = 30 r_g$.

central hole, it can intercept only a tiny fraction of the thermalized emission, if its size is comparable or smaller than the transition radius. This would produce much harder spectra than observed, $\Gamma < 1$. Therefore we choose here a weaker dependence, although the particular value of the exponent is chosen rather arbitrarily and no attempt is made here to tune it to the observed data. The slow dependence may be interpreted as the optically thick plasma slowly disappearing (disc disrupted into small clouds; covering factor gradually decreasing from 1 to 0) with decreasing r , or the emission coming from perturbations propagating in the entire volume of the hot plasma.

The emitting structures are assumed to originate at $r_{\text{out}} \geq r_{\text{tr}}$ at a mean rate of λ per second. Time intervals between the launch of successive flares are generated from the $\lambda \exp(-\lambda t)$ distribution, as appropriate for a Poissonian process. Each flare is followed until it reaches the marginally stable orbit at $r_{\text{ms}} = 6 r_g$. At each time step the primary Comptonized component and its reprocessed component are computed. The truncation radius is assumed $r_{\text{tr}} = 30 r_g$, so that the time average spectral slope of the Comptonized continuum is $\Gamma = 1.6\text{--}1.7$.

The Comptonized spectrum is computed using the code THCOMP (Zdziarski, Johnson & Magdziarz 1996), solving the Kompaneets equation. Computations are parametrized by the photon spectral index, which we compute from $\Gamma = 2.33(l_{\text{h}}/l_{\text{s}})^{-1/6}$ (Beloborodov 1999a,b), and electron temperature $kT_e/(m_e c^2)$ computed using formulae from Beloborodov (1999b). Plasma optical depth is assumed $\tau_{\text{es}} = 1.8$ (PF99).

The reprocessing medium is assumed to be ‘cold’, (only hydrogen and helium ionized) with elements abundances of Morrison & McCammon (1983). The spectrum of the Compton reflected continuum is computed from the simple formula of Lightman & White (1988),

$$S_{\text{refl}}(E) = \frac{1 - \epsilon}{1 + \epsilon} S_{\text{prim}}(E), \quad \epsilon = \sqrt{\frac{\kappa_{\text{abs}}}{\kappa_{\text{abs}} + \kappa_{\text{es}}}}, \quad (5)$$

where $\kappa_{\text{abs}}(E)$ and $\kappa_{\text{es}}(E)$ are the photo-absorption and electron scattering opacities, respectively. The above formula is multiplied by a simple exponential cutoff to mimic the high energy cutoff. This is sufficient for our purposes since only the spectra up to ≈ 30 keV will be considered. The Fe K α line is added to the reflected continuum, with equivalent

width (EW) as a function of Γ , following computations of Życki & Czerny (1994; see also Z02). Importantly, the instantaneous amplitude of the reprocessed component is assumed to depend on radius of emission,

$$R(r) = \begin{cases} 1 & \text{for } r > r_{\text{tr}} \\ \frac{r - r_{\text{ms}}}{r_{\text{tr}} - r_{\text{ms}}} & \text{for } r < r_{\text{tr}}, \end{cases} \quad (6)$$

i.e. it linearly decreases from 1 at $r = r_{\text{tr}}$ to 0 at $r = r_{\text{ms}}$. Again, the particular form of the function $R(r)$ for $r < r_{\text{tr}}$ is chosen rather arbitrarily, the general condition being that $R(r)$ decreases inwards. Time evolution of Γ and R during a flare is plotted in Fig 1b.

Thus created sequence of spectra is subject to standard analysis in the time and Fourier domains (see e.g. van der Klis 1995; Nowak et al. 1999; Poutanen 2001). In particular, the Fourier frequency resolved (f -resolved hereafter) spectra are computed according to the prescription given by Revnivtsev et al. (1999; see also Z02). The normalized power spectral density (PSD) is computed as

$$P_j = 2 \frac{T}{\bar{C}^2} |C_j|^2, \quad j = 0, \dots, N - 1 \quad (7)$$

$$C_j = \sum_{k=0}^{N-1} c_k e^{2\pi i f_j t_k}, \quad (8)$$

where the discrete frequencies $f_j \equiv j/T$ for $j = -N/2, \dots, N/2$; T is the total light curve time, \bar{C} is the mean count rate, while c_k are the number of counts in k -th time bin. The f -resolved spectrum at energy E_i and Fourier frequency f_j is then defined as

$$S(E_i, f_j) = \bar{C}_i \sqrt{P_i(f_j) \Delta f_j} = \sqrt{\frac{2|C_{i,j}|^2}{T} \Delta f_j}. \quad (9)$$

All computations are done assuming the central black hole mass $M = 10 M_{\odot}$.

3 RESULTS

3.1 The case of a single value of velocity of the active regions

In the simple case of a single value of β we do not expect the observed PSD to be reproduced, since the f^{-1} behaviour generally requires a distribution of parameters and/or correlations between flares (Lehto 1989, Lochner, Swank & Szymkowiak 1991). It is nevertheless instructive to study other observables from the model. The velocity proportionality coefficient was adopted $\beta = 0.02$ and $r_{\text{out}} = 60 r_g$, so that the duration of a flare is $t_{\text{trav}} \approx 0.5$ s, and the PSD peaks at 0.5–1 Hz. Fig. 2 shows the f -resolved spectra and time lags as functions of energy. The model predictions do not match well the observed trends. The time lags as a function of energy are independent of Fourier frequency, at least for $f \leq 1$ Hz, that is below the peak frequency of PSD. This contrasts the observed $\delta\tau(E)$, which shows longer lags at a given E , for lower f (Nowak et al. 1999). The logarithmic dependence of energy is true for any flare profile, if the change of spectral index during the flare, $\Delta\Gamma$, is small compared to time average Γ (Kotov et al. 2001). In the considered case $\Delta\Gamma \approx 0.8$, so it is not small compared to $\langle\Gamma\rangle \approx 1.7$, but the logarithmic dependence $\delta\tau(E) \propto \log E$ is still obeyed,

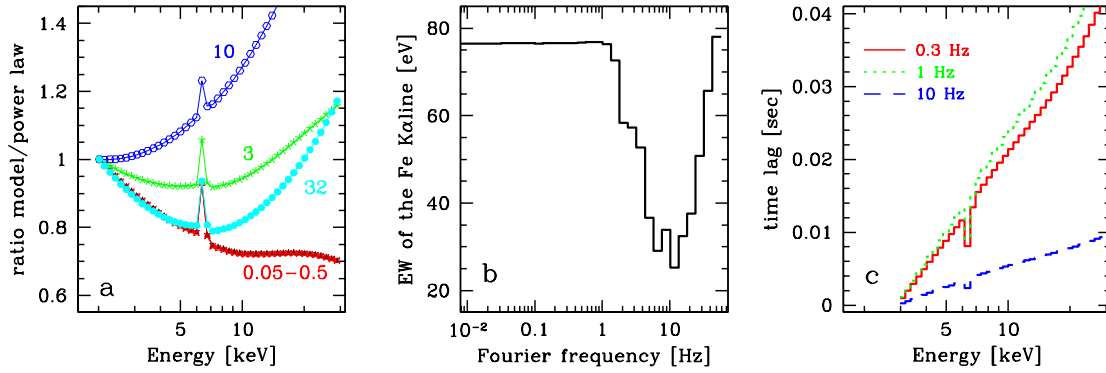


Figure 2. Results of simulations for a single value of active regions velocity. Parameters: $\beta = 0.02$, $r_{\text{out}} = 60 r_g$, so that the duration of a flare is $t_{\text{trav}} \approx 0.5$ s (Sec. 3.1). (a) The f -resolved spectra, divided by a power law, $N_E \propto E^{-1.6}$, and normalized to 1 at 2 keV (labels are middle frequencies in Δf_j in Hz as in equation 9) The spectra harden initially with f up to $f \sim 10$ Hz, then soften, with the corresponding increase of the reflection amplitude. (b) Equivalent width of the Fe K α line showing dependence on f matching that of the f -spectra. (c) Time lags as functions of energy, for three values of Fourier frequency (Kotov et al. 2001; also fig. 12 in Nowak et al. 1999).

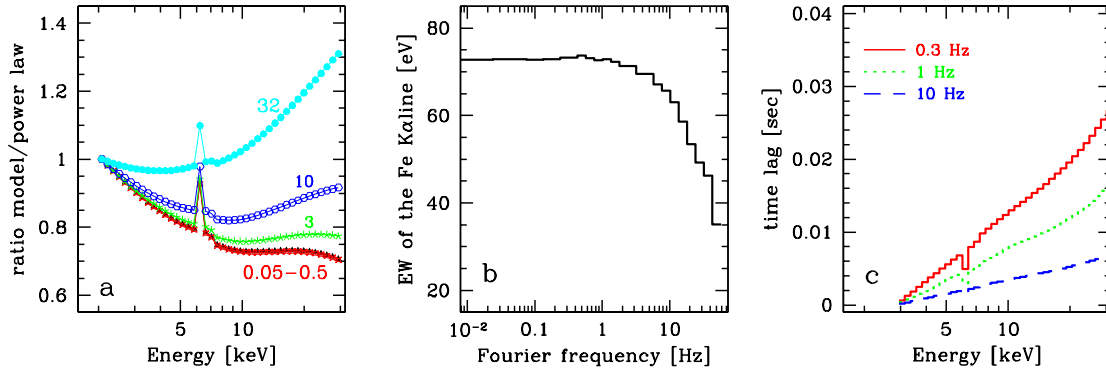


Figure 3. Results of simulations for avalanches of flares. Curves are described in the same way as in Fig. 2. Duration of the flares covers the range 0.03 s to 1.5 s ($\beta = 0.35$ –0.007, respectively). The f -resolved spectra and EW of K α line are now monotonic functions of Fourier frequency f , similarly to the observed dependencies (Revnivtsev et al. 1999). The $\delta\tau(E)$ dependence, panel (c), reproduces the observed dependencies well (compare with fig. 12 in Nowak et al. 1999).

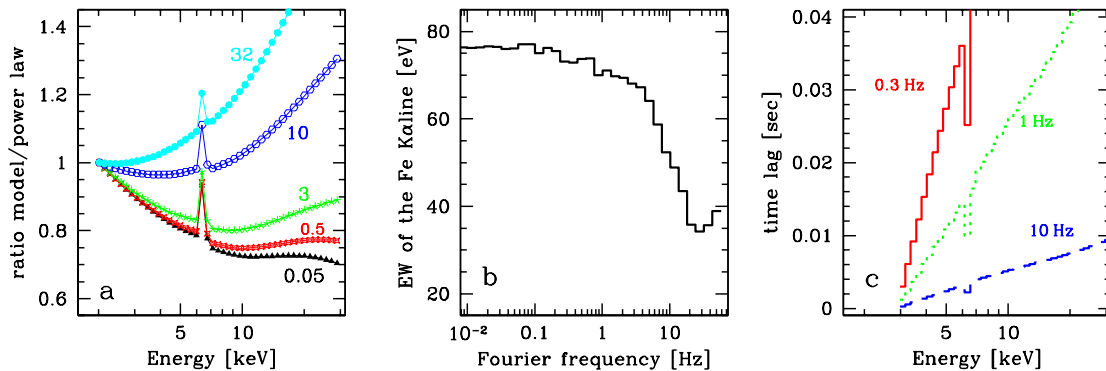


Figure 4. Results of simulations for a simple distribution of velocities of emission regions (no correlations between flares, i.e. no avalanches). Curves are described in the same way as in Fig. 2. The f -resolved spectra and EW of K α line are very similar to the avalanche case (Fig. 3), but the time lags $\delta\tau(E)$ are much longer and longer than those observed in Cyg X-1. Longer individual flares are necessary to generate variability power at frequencies down to 0.1 Hz.

at least for higher $f \geq 1$ Hz, and energies not exceeding ~ 30 keV. This is consistent with analytical solution, which can be obtained for a simple exponential profile and a linear dependence of $\Gamma(t)$. Assuming

$$S(E, t) = \exp(t/t_r) E^{-\Gamma_f + at}, \quad t < 0, \quad (10)$$

where Γ_f is the spectral index at the peak of a flare, at $t = 0$, the Fourier transform can be computed,

$$\hat{S}(E, f) = E^{-\Gamma_f} \frac{t_r}{1 - it_r 2\pi f + at_r \ln E}. \quad (11)$$

The phase lags are

$$\phi(f) \equiv \arg [\hat{S}(E_1, f) \hat{S}^*(E_2, f)], \quad (12)$$

where

$$\tan \phi(f) = \frac{-at_r^2 \ln(E_1/E_2) 2\pi f}{1 + at_r \ln(E_1 E_2) + a^2 t_r^2 \ln E_1 \ln E_2 + t_r^2 (2\pi f)^2}. \quad (13)$$

From this it can be seen that for small ϕ , the time lags $\delta\tau(E)$ are independent of f , $\delta\tau = \phi/(2\pi f) \approx \tan \phi/(2\pi f) \approx \text{const}$.

The dip in $\delta\tau(E)$ at the energy of the Fe $K\alpha$ line, seen in the real data, is reproduced by the model, confirming the result of Kotov et al. (2001).

The observed spectral slope of the comptonized continuum and the equivalent width of the Fe $K\alpha$ line are monotonic functions of f , at least above ≈ 0.5 Hz (Revnivtsev et al. 1999). In contrast to these, the model f -resolved spectra show complex dependence on f . In particular the EW of the $K\alpha$ line first decreases above ≈ 1 Hz, then increases again above ≈ 10 Hz. This means that in the Fourier decomposition of the flare profile the highest frequencies form the first part of the rising profile, which, in real space, is formed above the accretion disc (i.e. $r_{\text{tr}} < r < r_{\text{out}}$). The spectra from that part are soft, and the amplitude of reflection is close to 1. However, we note that the f -resolved spectra are dependent on the radial profile of the heating function (Eq. 2). Experimenting with the $l_h(r)$ function we find that a more peaked $l_h(r)$ (e.g. $\propto r^{-\gamma}$, $\gamma \geq 3$) produces the f -resolved spectra monotonically hardening with f and EW(f) monotonically decreasing.

3.2 Distribution of parameters

The full model obviously has to explain all observable characteristics of the X-ray emission. The complex but universal PSD of X-ray emission in low/hard state points out towards a universal mechanism of generating the complexity. One such mechanism was suggested by Stern & Svensson (1996) in the context of gamma-ray bursts and implemented by PF99 for accreting black holes. Their idea is that each flare can stimulate one or more flares to produce an 'avalanche' of many flares. Parameters of avalanches can be adjusted so that the power spectrum can have the observed slope of -1 (i.e. $P(f) \propto f^{-1}$) in a given frequency band.

The idea of avalanches of flares may be easily implemented in the present model. Different time-scales of individual flares correspond to different coefficients β , and the stimulated flares are assumed to originate from the same radius as the stimulating ones. Specifically, we assume that β follows a power law distribution $P(\beta) \propto \beta^k$ between β_1 and β_2 . There are λ spontaneous flares per second, and each

flare has a probability μ of stimulating a secondary flare, the latter being delayed by $t_{\text{delay}} = \alpha t_{\text{trav}}/7$, where t_{trav} is the duration of the stimulating flare, while α is drawn from a Poisson distribution of mean α_0 (the factor 7 approximately translates t_{trav} to flare time scale used by PF99; see there for detailed description of the model). The adopted values of the parameters are such that they give good description of PSD from black hole binaries: $k = 0.5$, $\beta_1 = 0.007$, $\beta_2 = 0.35$, $\lambda = 90$, $\mu = 0.7$, $\alpha_0 = 5$. The perturbations start from $r_{\text{out}} = 60 r_g$, so the duration of the flares cover the range from 0.03 to 1.5 sec.

Results for this model are presented in Figure 3. They match the observed dependencies reasonably well. Time lags as functions of energy are in good quantitative agreement with the observed values in the whole range of computed f (compare with Cyg X-1 data in Nowak et al. 1999). Interestingly, by superposing flares of different durations, the rising trend in EW(f) for $f > 10$ Hz (see Fig. 2) was compensated for, and the equivalent width is now monotonically decreasing with f . Correspondingly, the continuum hardens monotonically with f . Both trends are as observed in black hole binaries (Revnivtsev et al. 1999, 2001). This means that not only are higher frequencies formed from shorter flares, but within the flares the dominant contribution to a given f moves towards the peak of the flare, as f increases.

For comparison, Fig. 4 shows results obtained assuming a simple distribution of velocities of the emission structures (no correlations between flares). Coefficients β was drawn from a uniform distribution between $\beta_1 = 0.003$ and $\beta_2 = 0.1$ (flare durations 0.1 s to 3.5 s). Importantly, the lower value β_1 is now much smaller than that in the avalanche prescription, to give flat $P(f)$ down to ≈ 0.1 Hz. As a result, the time lags are now longer than those for avalanches, clearly longer than those observed.

3.3 Accretion disc with hot ionized skin

The presented propagation model can also be formulated in the geometry of an accretion disc extending down to the last stable orbit, with the X-ray emitting structures moving above the disc towards the center. As a result of irradiation by hard X-rays, the hot ionized skin will form on the disc (Rózańska & Czerny 1996; Nayakshin & Dove 2001). Making the same assumption about increasing luminosity of the moving flare as in Section 2 (equation 2), the result is obtained that the thickness of the hot skin, τ_{hot} , increases towards the center (Nayakshin 2000; Życki & Rózańska 2001). This reduces the effectiveness of reprocessing/thermalization as the flare progresses. This in turn leads to diminishing supply of soft photons for Comptonization and hardening of the continuum as a consequence. Simultaneously, the relative amplitude of the "cold" reprocessed component decreases, since fewer photons penetrate to the cold disc beneath the hot skin (e.g. Done & Nayakshin 2001; Życki & Rózańska 2001). Qualitatively, the situation is thus analogous to the disrupted disc scenario, and could reproduce observed trends of Γ and R with Fourier frequency. In this Section a quantitative analysis of the model is performed.

Basic model element is the spectral evolution during a single flare. Here the radial dependence of the disc illuminating flux, $F_{\text{irr}}(r)$, is crucial since it determines the

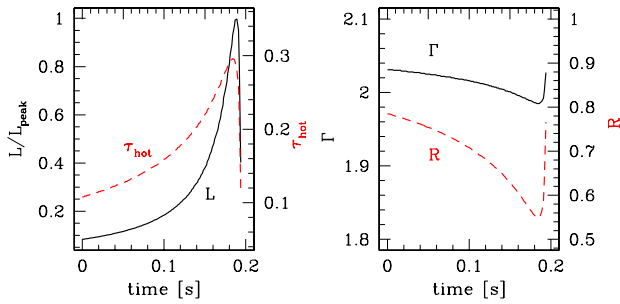


Figure 5. Time variations of parameters during a flare in the hot skin scenario (Sec. 3.3). Left panel: luminosity of a flare (solid curve) and the thickness of the hot skin (dashed curve), right panel: spectral index, Γ , and amplitude of reflection, R . Note the relatively small range of Γ and R , due to small variation of τ_{hot} . The spectral evolution during a flare is *insufficient* to produce correct hard X-ray time lags or f -resolved spectra.

$\tau_{\text{hot}}(r)$ dependence. The illuminating flux can be written as $F_{\text{irr}} = (\eta/\pi)L/(R_{\text{flare}}^2 + 3H^2)$, where $\eta \approx 0.5$ is the anisotropy factor, R_{flare} is the radius of a flare and H is its height above the disc (see PF99). Since, as argued above (equation 2), $L(r) \propto r^{-2}$, we would obtain $F_{\text{irr}}(r) \propto r^{-2}$ if $R_{\text{flare}} = \text{const}$ and $H = \text{const}$. However, for τ_{hot} to have a significant radial dependence, F_{irr} must be a stronger function of r . For example, for illumination due to local dissipation, $F_{\text{irr}}(r) \propto r^{-3}$. To achieve this, we assume here $R_{\text{flare}}(r) \propto H(r) \propto r^{1/2}$. That is, the flare shrinks and its height decreases as it approaches the center. The condition $R_{\text{flare}} \propto H$ is required in order to reproduce the Γ - R correlation, since it ensures that the geometry of the flare is constant and the only varying factor is the thickness of the hot skin. The proportionality coefficient in the $R_{\text{flare}}(r) = R_0 r^{1/2}$ relation can be computed if the maximum heating compactness, total source luminosity and flare occurrence rate are known (see eq. 7 in Z02).

Energy spectra during a flare are computed as in Z02. The thickness of the hot skin, τ_{hot} , is computed as a function of F_{irr} and r using the fitting formula (eq. 9) from that paper, while the amount of soft photons from thermalization re-entering an active region and the effective amplitude of reflection were computed from eqs. 3, 11 and 10 in Z02, respectively, following PF99 and Poutanen (2002). The feedback parameter $D_0 = 0.5$ (eq. 3 in Z02 and PF99)². The height H is assumed to be 0, so that in the absence of the hot skin $\Gamma \approx 2$. It should be emphasized that in the present scenario the time/radial dependencies of l_h/l_s and R can be predicted from physical considerations. Thus, eq. 4 and eq. 6 are *not* used here.

An example of a flare computed in this model is shown in Fig 5. The spectrum does evolve from soft to hard, but

² We note that the parametrization adopted by PF99 hides the fact that the required D_0 is actually incompatible with an emission region whose horizontal and vertical extent are comparable, if the emission is *isotropic*. According to PF99 for $D_0 = 0.5$ one half of the emitted X-rays return to the emission region if $H = 0$. This in reality implies the horizontal extent much larger than vertical one (slab-like geometry).

the change of Γ is very small, clearly insufficient to produce any difference in f -resolved spectra. A sequence of spectra was simulated, assuming a distribution of velocities of active regions and other parameters as in pulse avalanche prescription (Sec. 3.2). Computing the f -resolved spectra we confirm that they all have the same slope, $\Gamma \approx 2$, while the EW of the $K\alpha$ line is approximately constant at ≈ 55 eV. Thus, the hot skin disc model in the simple version considered here is not able to reproduce the f -resolved spectra.

The irradiation flux would have to be a very strong function of r for the hot skin thickness to increase enough to produce the required hard spectrum ($\Gamma \sim 1.6$ – 1.7 at the peak of the flare). This would mean a significant decrease of the size of the emitting region as it approaches the center, if the luminosity $L(r) \propto r^{-2}$ dependence is kept. That in turn would increase the compactness parameter, l_h , as well as the temperature of the soft thermalized radiation. The former cannot be uniquely constrained by the data, if the plasma is thermal (Maciolek-Niedźwiecki, Zdziarski & Coppi 1995), but the latter is observed to be no higher than $T_0 \sim 0.3$ keV (e.g. Di Salvo et al. 2001). It remains to be seen whether a physically plausible model can be constructed fulfilling all the constraints.

4 A MODEL COMPATIBLE WITH MULTI-LORENTZIAN DECOMPOSITION OF POWER SPECTRA

X-ray power spectra from accreting compact objects can be interpreted in terms of a (small) number of relatively narrow Fourier components (Nowak 2000; Belloni, Psaltis & van der Klis 2002). Higher quality data from RXTE clearly reveal that PSD, which were previously considered a roughly featureless power law with two or three breaks, consist of a number of peaks. This interpretation is strengthened by the correlations between frequencies of the components (Belloni et al. 2002), reducing the complexity of broad band variability to possibly just one parameter, at least within a given spectral state. The parameter seems to be related to the geometry of accretion flow, as evidenced by correlations between the characteristic frequencies and energy spectral properties (spectral slope, amplitude of the reprocessed component; Revnivtsev et al. 2001; Gilfanov et al. 2000). The obvious interpretation of the geometrical factor is the variable transition radius between the outer optically thick standard accretion disc and inner optically thin hot flow (Revnivtsev et al. 2001; Psaltis & Norman 2002).

The narrow components of PSD are usually modeled as Lorentz profiles. If the Lorentz profiles are taken seriously, the emission may be envisioned to consist of a collection of exponentially damped (or forced i.e. rising) harmonic oscillators. Obviously, the oscillations may be reduced to simple exponential shots, if the quality factor of the Lorentzians, $Q \sim \Delta f/f_0$ (f_0 is the resonant frequency while Δf is the half-width of the Lorentzian), is low enough, $Q \leq 1$. In the interpretation of Psaltis & Norman (2002), the frequencies would be connected to characteristic frequencies at the disc truncation radius: orbital, periastron-precession and nodal-precession (Stella & Vietri 1998). However, it is the hard X-ray emission that is actually variable, and the most likely reason for the variability is a variable energy dissipation

in the hot plasma, rather than variable input of soft photons (Maccarone et al. 2000; Malzac & Jourdain 2000), even though it is far from obvious how to make a connection between the disc frequencies and the energy dissipation in the hot plasma. Furthermore, hard X-ray time lags can be interpreted as a result of spectral evolution during individual emission events (shots/flares in the usual shot noise models; PF99; Kotov et al. 2001).

In this Section we consider a descriptive model compatible with the above ideas. Adopting the form of the Lorentzian function as in Nowak (2000),

$$P(f) = \pi^{-1} \frac{N^2 Q f_0}{f_0^2 + Q^2 (f - f_0)^2} \quad (14)$$

where N , Q and f_0 are amplitude, quality factor and resonant frequency of the oscillations, we simulate the shots of the following temporal profile:

$$A(t) = A_0 \exp\left(\frac{t}{t_r}\right) \cos(2\pi f_0 t + \phi_0), \quad t < 0. \quad (15)$$

Here, the normalization $A_0 = NQ^{1/2}$, the rise time $t_r = 2Q/(2\pi f_0)$ and ϕ_0 is a randomly chosen initial phase. Parameters of the Lorentzians are taken from fits to Cyg X-1 0–4 keV light curves (Table 2 in Nowak 2000). We ignore the lowest amplitude component QPO₂, which leaves us with 5 components.

The crucial assumption we make here is that the shots correspond to perturbations traveling through the plasma, from the truncation radius, r_{tr} , towards the center, at a speed which may, but does not need to be, the same for all components. In actual computations the speed is assumed constant in time, but assuming $v \propto v_{ff}$ (as in previous Sections) would not change our conclusions. The heating rate of the plasma is assumed to be proportional to the energy of the oscillations, i.e. $l_h(t) \propto [A(t)]^2$, as in usual oscillatory motion (the square of a damped/forced oscillator is again a damped/forced oscillator with a Lorentzian PSD). We emphasize that the heating is now *not* described by eq. 2, since it is determined by $A(t)$, but formulae for $l_s(t)$ and $R(t)$ (eq. 4 and eq. 6) are adopted. Each of the 5 components is chosen with the same probability, while the overall frequency of shots is adjusted to give the r.m.s. variability ≈ 30 percent. Computations of spectra and subsequent Fourier analysis proceeds as in previous models.

In the particular case considered here the longest $t_r \approx 1.2$ sec for the lowest f_0 component, and t_r is progressively shorter for the higher- f_0 components. The propagation speed, v , is chosen such that the travel time, $t_{trav} = (r_{tr} - r_f)/v$ is at least $5t_r$. This means that a shot is launched from r_{tr} at $t = -5t_r$, where t_r is the corresponding rise time-scale (the beginning of an exponential shot is obviously not well defined). The final minimum radius, r_f , reached at $t = 0$, is determined by v .

It is easy to predict qualitatively the results for f -resolved spectra, if the propagation speed is the same for all components. The higher the f_0 (the shorter the t_r), the shorter the distance traveled. Shorter distance means softer energy spectrum, since spectra produced closer to the truncation radius are, by construction, softer. Thus the f -resolved spectra can be expected to become softer with increasing f , opposite to those observed. Thus, obviously, a necessary condition for this model to reproduce the observed

f -spectra is to assume that the speed of the perturbations increases with f_0 . Then, the higher the frequency f , the farther from the cold disc the emission takes place, producing harder spectra. Adjusting the speeds accordingly we indeed obtain the required dependence of f -spectra (including EW of the K α line) on Fourier frequency.

5 DISCUSSION

We have considered a propagation model of X-ray variability in application to high energy emission from accreting compact objects. The motivation for our considerations comes from two directions: (1) problems faced by the models of localized flares (PF99) in explaining the f -resolved spectra (Z02), and (2) demonstration by Kotov et al. (2001) that a propagation model with spectral evolution can naturally explain the hard X-ray time lags. The model can be formulated in both considered geometries: truncated standard disc with inner hot flow and a standard disc with an active corona and the hot ionized skin. It should be emphasized, however, that the main parameters entering the spectral computations, $l_h/l_s(t)$ and $R(t)$ can be *predicted* only in the latter model, while they have to be assumed rather arbitrarily in the former. It is the greater predictive power of the hot skin scenario what enables to find unique model predictions and demonstrate the problems which the model faces.

Similar computations of variability could be performed in the context of the plasma outflow model of Beloborodov (1999a,b). Here the main parameter is the outflow speed. Qualitatively, the requirement for the model to work is that the speed increases inwards. A good physical model predicting the speed as a function of distance, X-ray flux and other parameters is necessary, in order to make quantitative predictions.

Let us concentrate now on the geometry of an inner hot X-ray producing flow with an outer standard optically thick disc. This is one of the possibilities of the geometrical arrangement of accreting multi-phase plasma. It naturally accounts for hard spectra of black hole X-ray binaries, small amplitude of the reprocessed component, and observed correlations between these spectral parameters (Done 2002 and references therein). Emission in the form of flares (shots) associated with active regions and/or perturbations traveling in the hot plasma might then be responsible for observed time and spectral variability, considering that X-ray variability is generally of stochastic character (Czerny & Lehto 1997). Such an extension of models of steady emission from hot flows (e.g. Esin, McClintock & Narayan 1997) is necessary, considering the many observable characteristics related to variability. The situation is fully analogous to models invoking active regions above an accretion disc (e.g. Stern et al. 1995). These models could explain the steady Comptonized emission by basically adjusting one parameter, the ratio of heating to cooling compactnesses. When supplemented with the idea of plasma outflow (Beloborodov 1999a,b) or a hot ionized skin (Nayakshin & Dove 2001), they could explain the diversity of spectra and correlations between spectral parameters. However, in order to explain the complex time variability, a number of additional features had to be added: correlations between flares (avalanches) to explain the PSD and spectral evolution during a flare as a

result of, e.g., rising the active region above the disc (PF99). Similar developments can be expected in the hot flow scenario.

Precise geometry of the X-ray emitting structures in the hot flow is obviously uncertain, but certain constraints can be obtained. For example, compact active regions (size much smaller than the inner disc radius) moving through hot plasma totally devoid of optically thick plasma (i.e. the cold disc sharply disrupted at certain radius), would intercept so few soft photons at $r < r_{\text{tr}}$ that the continuum slope would be much harder than observed. One possibility would then be that the active regions are compact but the disappearance of the optically thick phase is gradual, moving from r_{tr} inwards. This could mean that small optically thick clouds form inside the hot plasma at $r < r_{\text{tr}}$ and their filling factor gradually decreases inwards from ≈ 1 to 0. Detailed simulations would be necessary to predict spectra from such a configuration (e.g. Malzac & Celotti 2002). At a rather speculative level one might point out two possibilities of formation of such compact traveling active regions. The accreting plasma might form multiple shocks where the dissipation of energy would preferentially take place, or the active regions might have something to do with the dissipation of magnetic energy inside the hot flow, which dissipation is necessary to maintain the equipartition between the magnetic and thermal energy (Bisnovatyi-Kogan & Lovelace 2000).

Another possibility for the geometry is to assume that the disc is rather sharply truncated but the X-ray emission comes from global coherent perturbations propagating through the entire volume of the hot plasma. Then the decrease of l_s/l_h would roughly correspond to the decrease of the solid angle subtended by the cold disc, as the perturbation approaches the center.

Temporal profiles of the flares considered in this paper were rather simple, therefore to produce a broad band PSD a distribution of parameters (e.g. flare timescale) was required. One might envision more complex profiles based on, e.g., recent considerations of Maccarone & Coppi (2002). They suggest correlations between launch times of short flares ($t_r \approx 0.5$ sec), such that the short flares fill in a specific temporal envelope function. We note that their flares do not explain the whole range of time-scales, since the PSD above ~ 1 Hz is under-predicted. Even shorter flares would be necessary to generate enough power at sub-second time-scales, perhaps filling in the short flares considered by Maccarone & Coppi (2002) as envelopes. The result might then be equivalent to a hierarchical scenario proposed by Uttley & McHardy (2001), where a long time-scales perturbation propagate from outside, breaking down into smaller, faster structures in a fractal-like manner.

ACKNOWLEDGMENTS

This work was partly supported by grant no. 2P03D01718 of the Polish State Committee for Scientific Research (KBN).

REFERENCES

Belloni T., Psaltis D., van der Klis M., 2002, *ApJ*, 572, 392
 Beloborodov A. M., 1999a, *ApJ*, 510, L123

Beloborodov A. M., 1999b, in Poutanen J., Svensson R. eds, ASP Conf. Ser. 161, High Energy Processes in Accreting Black Holes, 295, (astro-ph/9901108)
 Bisnovatyi-Kogan G. S., Lovelace R. V. E., 2000, *ApJ*, 529, 978
 Böttcher M., Liang E. P., 1999, *ApJ*, 511, L37
 Czerny B., 2002, in Active Galactic Nuclei: from Central Engine to Host Galaxy, ASP Conference Series, Eds. S. Collin, F. Combes and I. Shlosman, in press
 Czerny B., Lehto H. J., 1997, *MNRAS*, 285, 365
 Di Salvo T., Done C., Życki P. T., Burderi L., Robba N. R., 2001, *ApJ*, 547, 1024
 Done C., 2002, *Philosophical Transactions of the Royal Society*, 360, 1967 (astro-ph/0203246)
 Done C., Nayakshin S., 2001, *MNRAS*, 328, 616
 Esin A. A., McClintock J. E., Narayan R., 1997, *ApJ*, 489, 865
 Gilfanov M., Churazov E., Revnivtsev M., 2000, Proc. 5th Sino-German Workshop on Astrophysics, SGSC Conference Ser., Vol. 1, China Science & Technology Press, Beijing, p. 114 (astro-ph/0002415)
 Kotov O., Churazov E., Gilfanov M., 2001, *MNRAS*, 327, 799
 Lehto H. J., 1989, in The 23rd ESLAB Symposium on Two Topics in X-Ray Astronomy. Volume 1: X Ray Binaries, ESA, p. 499
 Lightman A. P., White T. R., 1988, *ApJ*, 335, L57
 Lochner J. C., Swank J. H., Szymkowiak A. E., 1991, *ApJ*, 376, 295
 Maccarone T. J., Coppi P. S., 2002, *MNRAS*, in press (astro-ph/0204153)
 Maccarone T. J., Coppi P. S., Poutanen J., 2000, *ApJ*, 537, L107
 Maciotek-Niedźwiecki A., Zdziarski A. A., Coppi P. S., 1995, *MNRAS*, 276, 273
 Malzac J., Celotti A., 2002, *MNRAS*, 335, 23
 Malzac J., Jourdain E., 2000, *A&A*, 359, 843
 Miller K. A., Stone J. M., 2000, *ApJ*, 534, 398
 Miyamoto S., Kitamoto S., 1989, *Nat*, 342, 773
 Morrison R., McCammon D., 1983, *ApJ*, 270, 119
 Nayakshin S., 2000, *ApJ*, 534, 718
 Nayakshin S., Dove J. B., 2001, *ApJ*, 560, 885
 Nowak M. A., 2000, *MNRAS*, 318, 361
 Nowak M. A., Wilms J., Vaughan B. A., Dove J. B., Begelman M. C., 1999, *ApJ*, 515, 726
 Poutanen J., 2001, *AdSpR*, 28, 267 (astro-ph/0102325)
 Poutanen J., 2002, *MNRAS*, 332, 257
 Poutanen J., Fabian A. C., 1999, *MNRAS*, 306, L31 (PF99)
 Poutanen J., Krolik J. H., Ryde F., 1997, *MNRAS*, 292, L21
 Psaltis D., Norman C., 2002, *ApJ*, in press (astro-ph/0001391)
 Revnivtsev M., Gilfanov M., Churazov E., 1999, *A&A*, 347, L23
 Revnivtsev M., Gilfanov M., Churazov E., 2001, *A&A*, 380, 520
 Różańska A., Czerny B., 1996, *Acta Astron.*, 46, 233
 Różańska A., Czerny B., 2000, *A&A*, 360, 1170
 Shakura N. I., Sunyaev R. A., 1973, *A&A*, 24, 337
 Stella L., Vietri M., 1998, *ApJ*, 492, L59
 Stern B. E., Svensson R., 1996, *ApJ*, 469, L109
 Stern B. E., Poutanen J., Svensson R., Sikora M., Begelman M. C., 1995, *ApJ*, 449, L13
 Uttley P., McHardy I. M., 2001, *MNRAS*, 323, L26
 van der Klis M., 1995, in Lewin W. H. G., van Paradijs J., van den Heuvel E. P. J., eds, X-ray binaries, Cambridge Univ. Press, Cambridge, p. 252
 Zdziarski A. A., Johnson W. N., Magdziarz P., 1996 *ApJ*, 283, 193
 Zdziarski A. A., Lubiński P., Smith D. A., 1999, *MNRAS*, 303, L11
 Życki P. T., 2002, *MNRAS*, 333, 800 (Z02)
 Życki P. T., Czerny B., 1994, *MNRAS*, 266, 653
 Życki P. T., Różańska A., 2001, *MNRAS*, 325, 197